

# Sol-gel synthesis of mixed ferrites for biomedical applications

Joel Espino-Portillo\*, Dora A. Cortés-Hernández, José C. Escobedo-Bocardo, Héctor J. Sánchez, Mirna M. G. Saldívar-Ramírez, Laura E. De-León-Prado

Cinvestav-IPN, Unidad Saltillo, Ramos Arizpe, 25900, México

\*Corresponding author

DOI: 10.5185/amp.2018.906  
www.vbripress.com/amp

## Abstract

The effect of mixed ferrites nature and that of several coatings on the magnetic properties and thus, on the heating ability of nanoparticles, was studied. The  $Mg_{0.4}Ca_{0.6}Fe_2O_4$  and  $Mn_{0.5}Ga_{0.5}Fe_2O_4$  ferrites, synthesized by sol-gel method, followed by heat treatment, were coated with oleic acid + Pluronic® F-127, carboxymethyl-dextran sodium or polyvinylpyrrolidone. An average particle size of 12 and 15 nm was obtained for the Mg-Ca and Mn-Ga ferrites, respectively. Samples, before and after coating, revealed a heating capacity over 42°C and a superparamagnetic behaviour. The compounds accomplished the requirements of heating ability and specific absorption rate for magnetic hyperthermia treatment. The  $Mn_{0.5}Ga_{0.5}Fe_2O_4$  system was more efficient than the  $Mg_{0.4}Ca_{0.6}Fe_2O_4$  system. Copyright © 2018 VBRI Press.

**Keywords:** Sol-gel, magnetic nanoparticles, hyperthermia.

## Introduction

Specific magnetic nanoparticles (MNPs) are able to eliminate cancer cells by hyperthermia treatment, which consists in applying an external magnetic field to the nanoparticles that increases their temperature between 41 – 46 °C<sup>1,2</sup>. The efficiency of the heating capacity required for the treatment is evaluated with the specific absorption rate (SAR) value, which is the amount of energy converted into heat per time and mass<sup>3</sup>. Several methods, such as co-precipitation<sup>4</sup>, thermal decomposition<sup>5</sup>, sol-gel<sup>6</sup>, microwave-assisted synthesis<sup>7</sup>, etc., have been employed to synthesize MNPs. Sol-gel is an efficient and convenient method according to many studies, due to the elevated purity of synthesized MNPs, relatively low reaction temperature (25 – 200 °C), narrow size distribution of MNPs and low cost. Sol-gel has been used to synthesize many kinds of doped or co-doped magnetic oxides of Ga, Co, Mn, Ca, MnGa, Mg-Ca, Mg-Mn, Mg-Zn, Mn-Ga<sup>5,6,8-14</sup>. According to the literature, is possible to synthesize Mn-Ga and Mg-Ca ferrites able to be used like materials for biomedical applications<sup>13,8</sup>.

In this work, magnetic nanoparticles of  $Mn_{0.5}Ga_{0.5}Fe_2O_4$  and  $Mg_{0.4}Ca_{0.6}Fe_2O_4$  were synthesized by sol-gel followed by heat treatment and coated with three different materials: i) oleic acid + Pluronic® F-127 (OA&P), ii) carboxymethyl-dextran sodium (Dxt); or iii) polyvinylpyrrolidone (PVP). The aim was to evaluate and compare their heating ability and magnetic properties.

## Experimental

### Materials

Analytical grade chemicals (Sigma Aldrich) of iron (III) nitrate nonahydrate ( $Fe(NO_3)_3 \cdot 9H_2O$ ), magnesium nitrate hexahydrate ( $Mg(NO_3)_2 \cdot 6H_2O$ ), calcium nitrate tetrahydrate ( $Ca(NO_3)_2 \cdot 4H_2O$ ), manganese (II) nitrate tetrahydrate ( $Mn(NO_3)_2 \cdot 4H_2O$ ), gallium (III) nitrate hydrate, ( $Ga(NO_3)_3 \cdot H_2O$ ), and ethylene glycol ( $C_2H_6O_2$ ) were used.

### Preparation of magnetic nanoparticles

#### Sol-gel synthesis

Stoichiometric amounts of  $Mg(NO_3)_2 \cdot 6H_2O$ ,  $Ca(NO_3)_2 \cdot 4H_2O$ , and  $Fe(NO_3)_3 \cdot 9H_2O$  were mixed for obtaining the Mg-Ca precursor, while stoichiometric amounts of  $Mn(NO_3)_2 \cdot 4H_2O$ ,  $Ga(NO_3)_3 \cdot H_2O$ , and  $Fe(NO_3)_3 \cdot 9H_2O$  were mixed for obtaining the Mn-Ga precursor. Then, 5 mL of  $C_2H_6O_2$  were added to each mixture. To obtain the sol, the mixtures were stirred during 2 h at 40 °C. This sol was heated up to 80 °C until a polymeric gel was obtained. Each gel was aged at room temperature during 2 h. Finally, gels were dried in an oven at 95 °C for 72 h. The Mg-Ca precursor was heat treated of 350 °C for 30 min, while the Mn-Ga precursor was heated at 500 °C for 1 h<sup>8,13</sup>.

#### Coating process

The procedure for the oleic acid + Pluronic® F-127 (OA&P) coating process was based on the work reported

by Wright *et al.*<sup>15</sup>. MNPs were dispersed in 150 mL of deionized water, 2M KOH solution was used to increase pH and 2 mL of oleic acid were added to the suspension and the mixture was stirred during 45 min at 50 °C. Once the suspension was cooled at room temperature, particles were washed with acetone and dried in an oven at 95 °C. The oleic acid coated particles were dispersed in deionized water and 2 g of Pluronic® F-127 were added to the suspension. The mixture was sonicated in a water bath for 15 min and stirred during 20 h. Finally, particles were washed with deionized water. For the carboxymethyl-dextran sodium (Dxt) and the polyvinylpyrrolidone (PVP) coating processes, the procedure was as follows: the uncoated particles were dispersed in deionized water, then 2 g of the coating material were added and pH was increased using 2M KOH. The suspension was dispersed during 15 min and then it was sonicated at 500 rpm for 20 h at 45 °C. Then, the solution was washed and dried in a stove at 95 °C.

### Characterizations

Heat treated samples were characterized by X-ray diffraction (XRD, Philips X'Pert), thermogravimetric analysis (TGA, Perkin Elmer Pyris Diamond), transmission electron microscopy (TEM, Titan 80, 300 kV) and energy dispersive spectroscopy (EDS), vibrating sample magnetometry (VSM, MicroMag 2900), Fourier transform infrared spectroscopy (FTIR, Thermo Scientific Nicolet IS5), and solid state magnetic induction (EasyHeat 0224 Ambrell). The coated ferrites were analyzed by FTIR and solid state magnetic induction. The heating efficiency was calculated according to Eq. (1),

$$SAR = \frac{C}{m} * \frac{\Delta T}{\Delta t} \quad (1)$$

where  $C$  is the specific heat of the medium where the particles are suspended ( $H_2O = 4.18 \text{ Jg}^{-1}$ ),  $\Delta T / \Delta t$  is the slope of the temperature vs time curve and  $m$  is the ferrite mass in the fluid per unit mass of fluid.

### Results and discussion

The XRD patterns of  $Mn_{0.5}Ga_{0.5}Fe_2O_4$  and  $Mg_{0.4}Ca_{0.6}Fe_2O_4$  are shown in Fig. 1. For the Mg-Ca ferrite, the reflections closely match to those of the JCPDS 88-1935 card, their angles are slightly higher due the substitution of  $Ca^{2+}$  for  $Mg^{2+}$ . The reflections of Mn-Ga ferrite are nearly those of the JCPDS 74-2229 card and their angles are slightly lower. According to the literature, both reflections correspond to a cubic inverse spinel structure similar to that of magnetite<sup>16,17</sup>.

The thermal behavior of both compounds is presented in Fig. 2. The  $Mn_{0.5}Ga_{0.5}Fe_2O_4$  ferrite showed a total weight loss of 6 % while  $Mg_{0.4}Ca_{0.6}Fe_2O_4$  presented a total of 22 %. The first loss that presented both materials (below 100°C), was due the water evaporation. The second weight loss was due to the evaporation of the ethylene glycol, at 270°C for  $Mn_{0.5}Ga_{0.5}Fe_2O_4$  and at

300°C for  $Mg_{0.4}Ca_{0.6}Fe_2O_4$ . The third loss, at 550 and 680°C for  $Mg_{0.4}Ca_{0.6}Fe_2O_4$  and  $Mn_{0.5}Ga_{0.5}Fe_2O_4$ , respectively, corresponds to the remaining organic compound evaporation. The Mg-Ca ferrite presented a higher weight loss (22 %), this may be due to the fact that the heat treatment of this sample was performed at a lower temperature and for a shorter period of time than those used for the Mn-Ga ferrite.

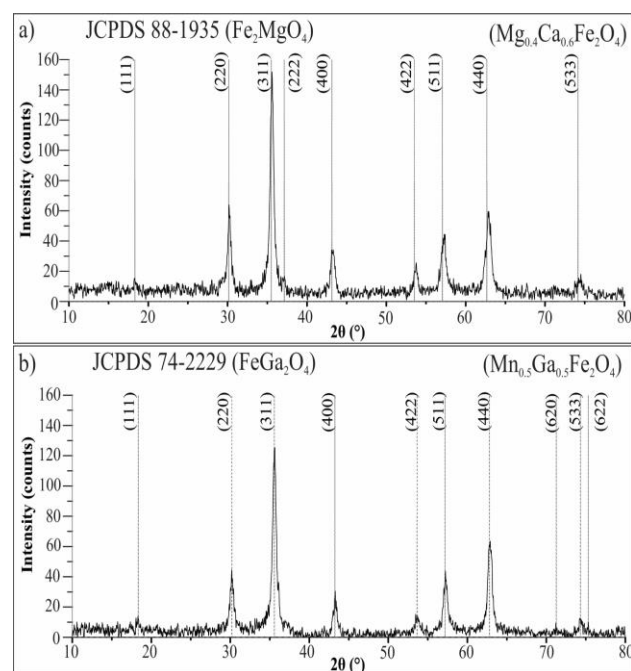


Fig. 1. XRD patterns of synthesized a)  $Mg_{0.4}Ca_{0.6}Fe_2O_4$  and b)  $Mn_{0.5}Ga_{0.5}Fe_2O_4$  samples.

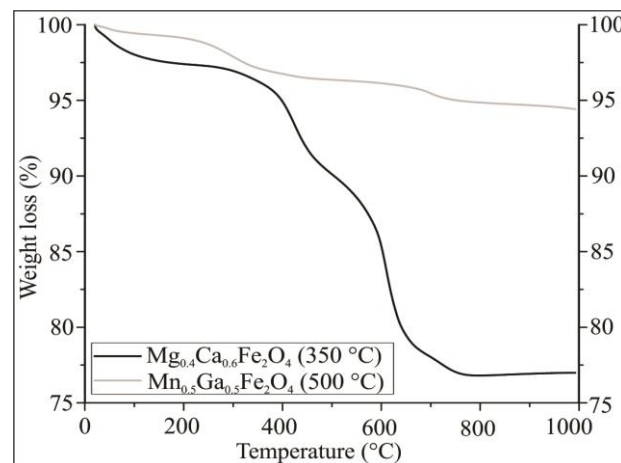
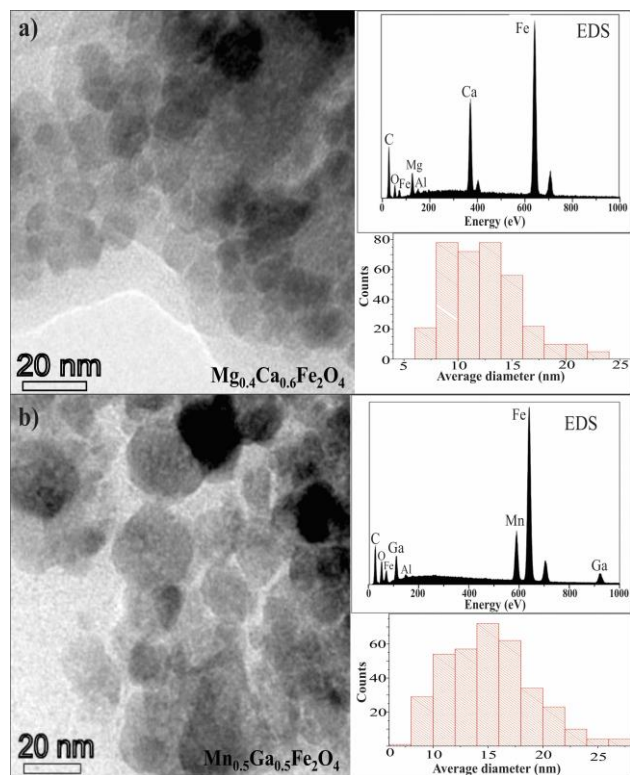


Fig. 2. Thermogravimetric spectra of magnetic nanoparticles samples.

The TEM images, EDS spectrum and average particle size of both ferrites are shown in Fig. 3. The morphology of the nanoparticles tends to be spherical; the EDS results indicated the presence of Fe, Mg and Ca for  $Mg_{0.4}Ca_{0.6}Fe_2O_4$  and Fe, Ga and Mn for  $Mn_{0.5}Ga_{0.5}Fe_2O_4$ , which indicates the purity of the synthesized materials. Based on 350 measurements for each system, the average particle size was of  $12 \pm 3.46 \text{ nm}$  for the Mg-Ca ferrite and  $15 \pm 3.87 \text{ nm}$  for the Mn-Ga ferrite.



**Fig. 3.** TEM images, EDS spectra and histograms of a)  $\text{Mg}_{0.4}\text{Ca}_{0.6}\text{Fe}_2\text{O}_4$  and b)  $\text{Mn}_{0.5}\text{Ga}_{0.5}\text{Fe}_2\text{O}_4$  samples.

The magnetic behavior of both ferrites is shown in **Fig. 4**. The Mn-Ga ferrite showed a higher saturation magnetization ( $M_s$ ) than the Mg-Ca ferrite, however this Mg-Ca ferrite showed no remnant magnetization ( $M_r$ ) and no coercive field ( $H_c$ ). This indicates that the Mn-Ga ferrite has a nearly superparamagnetic behavior, while the Mg-Ca ferrite is superparamagnetic.

The FTIR spectra of both ferrites, before and after coating, are shown in **Fig. 5**. Before coating, the existence of bands at about  $540\text{ cm}^{-1}$  (and at  $875\text{ cm}^{-1}$  for the Mg-Ca ferrite), demonstrate the M-O bonds of the ferrite. Around  $1320$ ,  $1410$  and  $2300\text{ cm}^{-1}$  were identified the bands of C-O group that belongs at the remnant ethylene glycol,  $\text{NO}_3^-$  from the precursors and  $\text{CO}_2$  atmospheric, respectively. For the oleic acid + Pluronic<sup>®</sup> F-127 coated ferrites, three bands at  $1100$ ,  $1450$  and  $2900\text{ cm}^{-1}$  were identified, which are representative of the Pluronic<sup>®</sup> F-127 that is chemically bonded to the oleic acid, the symmetrical stretching vibrations of the C=O group indicates the chemical bond between the oleic acid and the surface of the ferrite, and the absorption band of the C-H group corresponds to the oleic acid. For the case of the carboxymethyl-dextran sodium coating, the existence of the bands around  $1020$ ,  $1600$  and  $2920\text{ cm}^{-1}$  were observed, these bands correspond to the C-O groups from carboxymethyl-dextran molecule, the  $-\text{C}(=\text{O})-\text{N}-\text{H}$  secondary bond indicates the functionalization of MNPs and characteristic asymmetric  $-\text{CH}_2$  stretching. For the PVP coating, the energy bands were localized around  $1421$  and  $1620\text{ cm}^{-1}$ , that correspond to the asymmetric bending vibrations of  $\text{CH}_2$  and the C=O group of PVP.

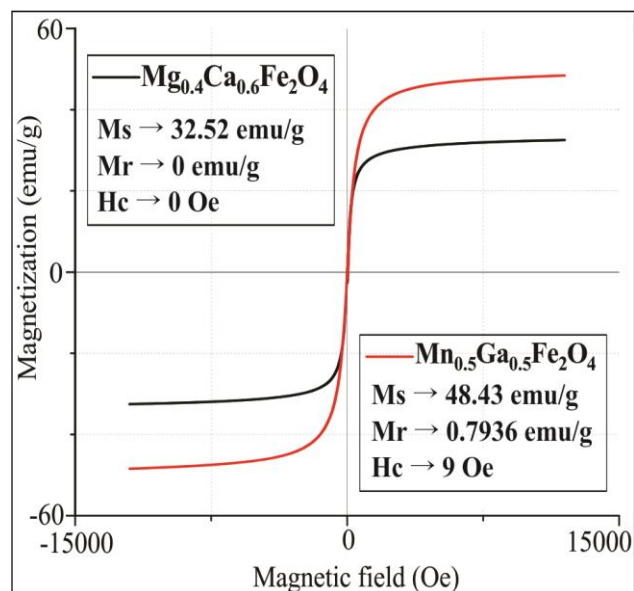


**Fig. 4.** Magnetic behavior of  $\text{Mg}_{0.4}\text{Ca}_{0.6}\text{Fe}_2\text{O}_4$  and  $\text{Mn}_{0.5}\text{Ga}_{0.5}\text{Fe}_2\text{O}_4$  ferrites.

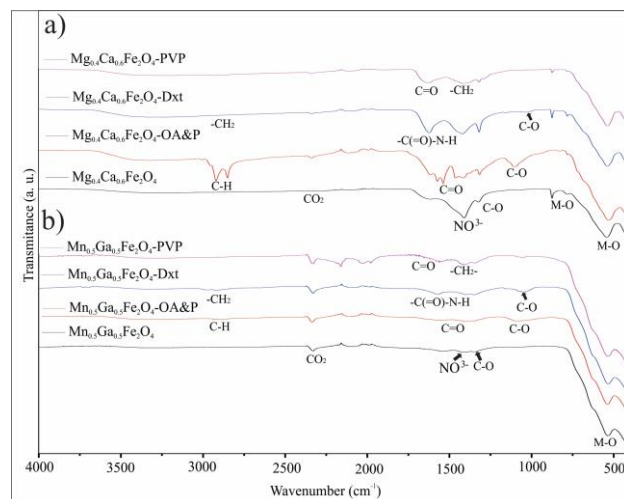


**Fig. 5.** FTIR spectra of a)  $\text{Mg}_{0.4}\text{Ca}_{0.6}\text{Fe}_2\text{O}_4$  and b)  $\text{Mn}_{0.5}\text{Ga}_{0.5}\text{Fe}_2\text{O}_4$  before and after coating with OA&P, Dxt and PVP.

According to **Fig. 6**, for aqueous suspensions of  $6\text{ mg/mL}$  and  $4\text{ mg/mL}$  for uncoated Mg-Ca and Mn-Ga ferrites, respectively, a temperature of  $42\text{ }^\circ\text{C}$  in  $10\text{ min}$  is achieved. As expected, temperature increases as the amount of ferrite mass is increased. For the case of the coated nanoparticles, all of them (measured with a mass of  $10\text{ mg/mL}$ ) can reach the minimal temperature required for hyperthermia in less than  $10\text{ min}$ . For both ferrites, the oleic acid + Pluronic<sup>®</sup> F-127 is the coating that leads to a higher decrease in heating ability, probably due to the use of a double coating. The PVP coating decreases the maximum temperature reached for the Mg-Ca ferrite suspension in approximately  $5\%$ , while for the Mn-Ga ferrite suspension the decrease is less than  $1\%$ . The Dxt coating showed no decrease in temperature for both systems. It is possible that the Dxt and PVP coatings decreased the agglomeration degree.

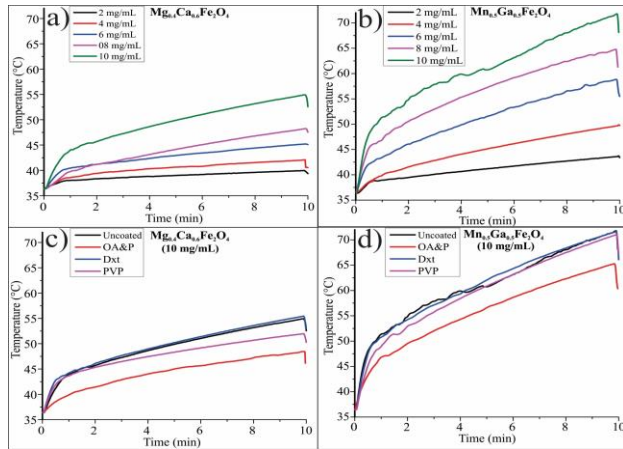


**Fig. 6.** Solid state magnetic induction of uncoated a) Mg<sub>0.4</sub>Ca<sub>0.6</sub>Fe<sub>2</sub>O<sub>4</sub>, b) Mn<sub>0.5</sub>Ga<sub>0.5</sub>Fe<sub>2</sub>O<sub>4</sub> and coated c) Mg<sub>0.4</sub>Ca<sub>0.6</sub>Fe<sub>2</sub>O<sub>4</sub> and d) Mn<sub>0.5</sub>Ga<sub>0.5</sub>Fe<sub>2</sub>O<sub>4</sub> ferrites.

According to **Table 1**, the SAR values for the Mn-Ga ferrites are higher than those of Mg-Ca ferrites. The highest SAR value for the Mg-Ca ferrite corresponds to the uncoated nanoparticles, followed by the Dxt coated nanoparticles. For Mn-Ga ferrite, the highest values correspond to the Dxt and PVP coatings. These data reinforce the idea that these coatings are decreasing the agglomeration of nanoparticles. However, a further research needs to be performed.

**Table 1.** SAR values of Mg<sub>0.4</sub>Ca<sub>0.6</sub>Fe<sub>2</sub>O<sub>4</sub> and Mn<sub>0.5</sub>Ga<sub>0.5</sub>Fe<sub>2</sub>O<sub>4</sub> samples before and after coating.

	Mg <sub>0.4</sub> Ca <sub>0.6</sub> Fe <sub>2</sub> O <sub>4</sub>		Mn <sub>0.5</sub> Ga <sub>0.5</sub> Fe <sub>2</sub> O <sub>4</sub>		
	$\Delta T/t / \Delta$	SAR (W/g)	$\Delta T/t / \Delta$	SAR (W/g)	
Uncoated	1.3816	289.22	Uncoated	2.4706	517.2
OA&P	1.0129	212.04	OA&P	2.2866	478.68
Dxt	1.3711	287.03	Dxt	2.5736	538.76
PVP	1.0369	217.06	PVP	2.6746	559.9

## Conclusion

Magnetic nanoparticles of Mg<sub>0.4</sub>Ca<sub>0.6</sub>Fe<sub>2</sub>O<sub>4</sub> and Mn<sub>0.5</sub>Ga<sub>0.5</sub>Fe<sub>2</sub>O<sub>4</sub> were successfully synthesized by sol-gel method. Both materials presented a single cubic inverse spinel structure. The magnetic nanoparticles showed a nearly spherical morphology with an average diameter of 12 and 15 nm for Mg-Ca and Mn-Ga ferrites, respectively. Remnant magnetization and coercive field values demonstrated a superparamagnetic behavior of both ferrites. The FTIR results demonstrated that it was possible to functionalize the ferrites surface with the oleic acid + Pluronic® F-127, carboxymethyl-dextran sodium or polyvinylpyrrolidone coatings. The heating ability required for hyperthermia applications of coated and uncoated ferrite suspensions, containing 10 mg of ferrite/mL of deionized water, was demonstrated.

## Acknowledgements

The authors gratefully acknowledge CONACyT Mexico the Master scholarship granted to Joel Espino Portillo (587639) and the research grants 222755 and 23025.

## Author's contributions

Conceived the plan: JEP, DCH, JEB; Performed the experiments: JEP, HS, MSR; Data analysis: JEP, DCH, JEB, HJS, MSR, LDP; Wrote the paper: JEP, DCH, JEB. Authors have no competing financial interests.

## References

- Tran, N. & Webster, T. J. Magnetic nanoparticles: biomedical applications and challenges. *J. Mater. Chem.* **20**, 8760 (2010). DOI: [10.1039/c0jm00994f](https://doi.org/10.1039/c0jm00994f)
- Baronzio, G. & Hager, E. *Hyperthermia in cancer treatment: a primer. Hyperthermia In Cancer Treatment: A Primer 1*, (Springer US, 2006). DOI: [10.1007/978-0-387-33441-7](https://doi.org/10.1007/978-0-387-33441-7)
- Pankhurst, Connolly, J., Jones, S. K. & J, D. Applications of magnetic nanoparticles in biomedicine. *J. Phys. D ...* **12**, (2003). (available at <http://iopscience.iop.org/0022-3727/36/13/201>).
- Cheng, F. Y. *et al.* Characterization of aqueous dispersions of Fe<sub>3</sub>O<sub>4</sub> nanoparticles and their biomedical applications. *Biomaterials* **26**, 729–738 (2005). DOI: [10.1016/j.biomaterials.2004.03.016](https://doi.org/10.1016/j.biomaterials.2004.03.016)
- De-León-Prado, L. E. *et al.* Synthesis and characterization of nanosized MgxMn1-xFe2O4 ferrites by both sol-gel and thermal decomposition methods. *J. Magn. Magn. Mater.* **427**, 230–234 (2017). DOI: [10.1016/j.jmmm.2016.11.036](https://doi.org/10.1016/j.jmmm.2016.11.036)
- Zhang, L. & Wu, Y. Sol-Gel Synthesized Magnetic MnFe<sub>2</sub>O<sub>4</sub> Spinel Ferrite Nanoparticles as Novel Catalyst for Oxidative Degradation of Methyl Orange. **2013**, (2013). DOI: [10.1155/2013/640940](https://doi.org/10.1155/2013/640940)
- Ahmad, R. *et al.* Improved electrical properties of cadmium substituted cobalt ferrites nano-particles for microwave application. *J. Magn. Magn. Mater.* **405**, 28–35 (2016). DOI: [10.1016/j.jmmm.2015.12.019](https://doi.org/10.1016/j.jmmm.2015.12.019)
- Sánchez, J. *et al.* Sol-gel synthesis of MnxGa1-xFe2O4 nanoparticles as candidates for hyperthermia treatment. *Solid State Sci.* **42**, 13755–13760 (2016). DOI: [10.1016/j.solidstatesciences.2013.07.010](https://doi.org/10.1016/j.solidstatesciences.2013.07.010)
- Sato Turtelli, R. *et al.* Interplay between the cation distribution and production methods in cobalt ferrite. *Mater. Chem. Phys.* **132**, 832–838 (2012). DOI: [10.1016/j.matchemphys.2011.12.020](https://doi.org/10.1016/j.matchemphys.2011.12.020)
- Jasso-Terán, R. A. *et al.* Synthesis, characterization and hemolysis studies of Zn(1-x)Ca(x)Fe2O4 ferrites synthesized by sol-gel for hyperthermia treatment applications. *J. Magn. Magn. Mater.* **427**, 241–244 (2017). DOI: [10.1007/s10856-014-5180-x](https://doi.org/10.1007/s10856-014-5180-x)
- Reyes-Rodríguez, P. Y. *et al.* Structural and magnetic properties of Mg-Zn ferrites (Mg1-xZnxFe2O4) prepared by sol-gel method. *J. Magn. Magn. Mater.* **427**, 268–271 (2017). DOI: [10.1016/j.jmmm.2016.10.078](https://doi.org/10.1016/j.jmmm.2016.10.078)
- Escamilla-Pérez, a. M., Cortés-Hernández, D. a., Almanza-Robles, J. M., Mantovani, D. & Chevallier, P. Crystal structure of superparamagnetic Mg0.2Ca0.8Fe2O4 nanoparticles synthesized by sol-gel method. *J. Magn. Magn. Mater.* **374**, 474–478 (2015). DOI: [10.1016/j.jmmm.2014.08.086](https://doi.org/10.1016/j.jmmm.2014.08.086)
- Saldívar-Ramírez, M. M. G. *et al.* Study on the efficiency of nanosized magnetite and mixed ferrites in magnetic hyperthermia. *J. Mater. Sci. Mater. Med.* **25**, 2229–2236 (2014). DOI: [10.1007/s10856-014-5187-3](https://doi.org/10.1007/s10856-014-5187-3)
- Sulaiman, N. H., Ghazali, M. J., Majlis, B. Y., Yunas, J. & Razali, M. Superparamagnetic calcium ferrite nanoparticles synthesized using a simple sol-gel method for targeted drug delivery. *Biomed. Mater. Eng.* **26**, S103–S110 (2015). DOI: [10.3233/BME-151295](https://doi.org/10.3233/BME-151295)
- Bolden, N. W., Rangari, V. & Jeelani, S. Synthesis of drug loaded iron oxide nanoparticles. in *ICCM International Conferences on Composite Materials* (2009).
- Maensiri, S., Sangmanee, M. & Wiengmoon, A. Magnesium Ferrite (MgFe2O4) Nanostructures Fabricated by Electrospinning. *Nanoscale Res. Lett.* **4**, 221 (2008). DOI: [10.1007/s11671-008-9229-y](https://doi.org/10.1007/s11671-008-9229-y)
- Weng, C.-H., Huang, C.-C., Yeh, C.-S., Lei, H.-Y. & Lee, G.-B. Synthesis of hollow, magnetic Fe/Ga-based oxide nanospheres using a bubble templating method in a microfluidic system. *Microfluid. Nanofluidics* **7**, 841 (2009). DOI: [10.1007/s10404-009-0442-5](https://doi.org/10.1007/s10404-009-0442-5)